PROCEEDINGS OF SCIENCE

A scoto-seesaw model with flavor symmetry

Joy Ganguly,[a,b] **Janusz Gluza**[c] **and Biswajit Karmakar**[c,*]

[a] *Department of Physics, Indian Institute of Technology Hyderabad, Telenagana, India*
[b] *Department of BSH, University of Engineering and Management, New Town, Kolkata, India*
[c] *Institute of Physics, University of Silesia in Katowice, Poland*

E-mail: biswajit.karmakar@us.edu.pl

We analyze a hybrid scoto-seesaw model based on the A_4 discrete symmetry to understand neutrino masses and mixing. The minimal type-I seesaw generates tribimaximal neutrino mixing at the leading order. The scotogenic contribution deviates from this first-order approximation of the lepton mixing matrix to yield the observed non-zero θ_{13} and to accommodate a potential dark matter candidate.

41st International Conference on High Energy Physics
6-13 July 2022, Bologna, Italy

*Speaker

https://pos.sissa.it/

PoS(ICHEP2022)1212

1. Introduction

In a scoto-seesaw framework [1, 2], it was shown that the minimal seesaw contribution can reproduce the tribimaximal (TBM) neutrino mixing with A_4 discrete flavor symmetry. Subsequently, a scotogenic contribution provides adequate deviation from TBM mixing, establishing a common origin of the nonzero θ_{13} and cosmological dark matter. Inclusion of the scotogenic contribution to the neutrino mass helps in reproducing the trimaximal (TM_2) mixing and generating the observed value of the reactor mixing angle θ_{13}. It also naturally incorporates dark matter candidates (three potential dark matter candidates, such as the dark fermion and real and imaginary components of the scalar field involved in the scotogenic contribution) into the picture. The model predicts the atmospheric mixing angle, Dirac and Majorana CP phases, and the effective mass parameter appearing in the neutrinoless double beta decay.

2. Structure of the model

Here we work in a hybrid scoto-seesaw framework [1, 2] with usual scotogenic fermion f and scalar doublet η, supported additionally by the A_4 discrete flavor symmetry and two right-handed neutrinos $N_{R_{1,2}}$. To obtain the flavor structure of the Yukawa couplings the flavons $\phi_s, \phi_a, \phi_T, \xi$ are introduced. The inclusion of flavon fields (SM gauge singlets) is a characteristic feature of models with discrete flavor symmetries [3–9]. Interestingly, the model contains an intrinsic $\mathbf{Z}_2$ symmetry under which both f and η are odd. The stability of the dark matter is ensured by this $\mathbf{Z}_2$ symmetry. In Table 1, we present transformation properties of all the fields content of our model under the complete discrete flavor symmetry. With fields content in Table 1, the charged lepton mass matrix

Fields	e_R, μ_R, τ_R	L_α	H	N_{R_1}	N_{R_2}	f	η	ϕ_s	ϕ_a	ϕ_T	ξ
A_4	$1, 1'', 1'$	3	1	1	1	1	1	3	3	3	$1''$
Z_4	$-i$	$-i$	1	-1	1	1	1	i	$-i$	1	-1
Z_3	ω	ω	ω^2	1	1	1	ω^2	1	1	ω	1
Z_2	-1	1	1	1	-1	-1	1	1	-1	-1	-1

Table 1: Field contents and transformation under the symmetries of our model.

is found to be diagonal. The Lagrangian that generates neutrino mass at a tree level by the type-I seesaw mechanism is given by

$$\mathcal{L}_N = \frac{y_{N_1}}{\Lambda}(\bar{L}\phi_s)\tilde{H}N_{R_1} + \frac{y_{N_2}}{\Lambda}(\bar{L}\phi_a)\tilde{H}N_{R_2} + \frac{1}{2}M_{N_1}\bar{N}^c_{R_1}N_{R_1} + \frac{1}{2}M_{N_2}\bar{N}^c_{R_2}N_{R_2} + h.c., \tag{1}$$

where $y_{N_{1,2}}$ are the corresponding couplings and $M_{N_{1,2}}$ are the Majorana masses of right-handed neutrinos. To get the flavor structure, we assume that the flavon fields get VEVs along $\langle\phi_s\rangle = (0, v_s, -v_s)$, $\langle\phi_a\rangle = (v_a, v_a, v_a)$ [10]. With these flavon VEVs, the Dirac and Majorana mass matrices are found to be

$$M_D = \frac{v}{\Lambda}\begin{pmatrix} 0 & y_{N_2}v_a \\ -y_{N_1}v_s & y_{N_2}v_a \\ y_{N_1}v_s & y_{N_2}v_a \end{pmatrix} = vY_N, \quad M_R = \begin{pmatrix} M_{N_1} & 0 \\ 0 & M_{N_2} \end{pmatrix}. \tag{2}$$

Now using the type-I seesaw formula the light neutrino mass matrix at the leading order can be written as

$$(M_\nu)_{\rm TREE} = -\begin{pmatrix} B & B & B \\ B & A+B & -A+B \\ B & -A+B & A+B \end{pmatrix}, \quad A = \frac{v^2 v_s^2 y_{N_1}^2}{\Lambda^2 M_{N_1}}, \quad B = \frac{v^2 v_a^2 y_{N_2}^2}{\Lambda^2 M_{N_2}}, \tag{3}$$

which can be diagonalized by TBM mixing matrix [11]. The scotogenic contribution in our model with the fermion f and scalar field η can be written as

$$\mathcal{L}_S = \frac{y_s}{\Lambda^2}(\bar{L}\phi_s)\xi i\sigma_2\eta^* f + \frac{1}{2}M_f \bar{f}^c f + h.c., \tag{4}$$

where y_s is the coupling and M_f is the mass of f. The VEV of ϕ_s and the non-trivial A_4 singlet ξ (which provides appropriate A_4 contraction) crucially dictate the structure of the scotogenic contribution and help in breaking the TBM mixing [12–16]. Therefore the contribution in the effective neutrino mass matrix originated from the scotogenic radiative corrections is given by [2, 17, 18]

$$(M_\nu)_{\rm LOOP} = \mathcal{F}(m_{\eta_R}, m_{\eta_I}, M_f) M_f Y_f^i Y_f^j, \text{ where} \tag{5}$$

$$\mathcal{F}(m_{\eta_R}, m_{\eta_I}, M_f) = \frac{1}{32\pi^2}\left[\frac{m_{\eta_R}^2 \log\left(M_f^2/m_{\eta_R}^2\right)}{M_f^2 - m_{\eta_R}^2} - \frac{m_{\eta_I}^2 \log\left(M_f^2/m_{\eta_I}^2\right)}{M_f^2 - m_{\eta_I}^2}\right], \tag{6}$$

where m_{η_R} and m_{η_I} are the masses of the neutral component of η. Once the flavons ϕ_s and ξ acquire VEVs in the direction $\langle\phi_s\rangle = (0, v_s, -v_s)$ and $\langle\xi\rangle = v_\xi$ respectively, the associated couplings can be written as $Y_F = (Y_F^e, Y_F^\mu, Y_F^\tau)^T = (y_s \frac{v_s}{\Lambda}\frac{v_\xi}{\Lambda}, 0, -y_s\frac{v_s}{\Lambda}\frac{v_\xi}{\Lambda})^T$. Finally, combining both contributions, the effective light neutrino mass matrix and the corresponding diagonalization matrix reads

$$\begin{aligned} M_\nu &= (M_\nu)_{\rm TREE} + (M_\nu)_{\rm LOOP} \\ &= \begin{pmatrix} -B+C & -B & -B-C \\ -B & -(A+B) & A-B \\ -B-C & A-B & -A-B+C \end{pmatrix}; U_\nu = \begin{pmatrix} \sqrt{\frac{2}{3}}\cos\theta & \frac{1}{\sqrt{3}} & \sqrt{\frac{2}{3}}e^{i\phi}\sin\theta \\ -\frac{\cos\theta}{\sqrt{6}} + \frac{e^{i\phi}\sin\theta}{\sqrt{2}} & \frac{1}{\sqrt{3}} & -\frac{\cos\theta}{\sqrt{2}} - \frac{e^{i\phi}\sin\theta}{\sqrt{6}} \\ -\frac{\cos\theta}{\sqrt{6}} - \frac{e^{i\phi}\sin\theta}{\sqrt{2}} & \frac{1}{\sqrt{3}} & \frac{\cos\theta}{\sqrt{2}} - \frac{e^{i\phi}\sin\theta}{\sqrt{6}} \end{pmatrix} U_m, \end{aligned} \tag{7}$$

where $U_m = {\rm diag}(1, e^{i\alpha_{21}/2}, e^{i\alpha_{31}/2})$ is the Majorana phase matrix. Without loss of generality we can write $A = |A|e^{i\phi_A}$, $B = |B|e^{i\phi_B}$, $C = |C|e^{i\phi_C}$. Now, let us define $\alpha = |A|/|C|$ and $\beta = |B|/|C|$, and phase differences $\phi_{AC} = \phi_A - \phi_C$ and $\phi_{BC} = \phi_B - \phi_C$. Hence θ and ϕ can be expressed in terms of model parameters as

$$\tan\phi = \frac{\alpha\sin\phi_{AC}}{1-\alpha\cos\phi_{AC}}, \quad \tan 2\theta = \frac{\sqrt{3}}{\cos\phi + 2\alpha\cos(\phi_{AC}+\phi)}. \tag{8}$$

Further comparing U_ν as given in Eq. (7) with U_{PMNS}, we find the following relations for mixing angles and $\delta_{\rm CP}$ as a function of θ and ϕ as [12]

$$\sin\theta_{13}e^{-i\delta_{\rm CP}} = \sqrt{\frac{2}{3}}e^{-i\phi}\sin\theta; \tan^2\theta_{23} = \frac{\left(1 + \frac{\sin\theta_{13}\cos\phi}{\sqrt{2-3\sin^2\theta_{13}}}\right)^2 + \frac{\sin^2\theta_{13}\sin^2\phi}{(2-3\sin^2\theta_{13})}}{\left(1 - \frac{\sin\theta_{13}\cos\phi}{\sqrt{2-3\sin^2\theta_{13}}}\right)^2 + \frac{\sin^2\theta_{13}\sin^2\phi}{(2-3\sin^2\theta_{13})}}. \tag{9}$$

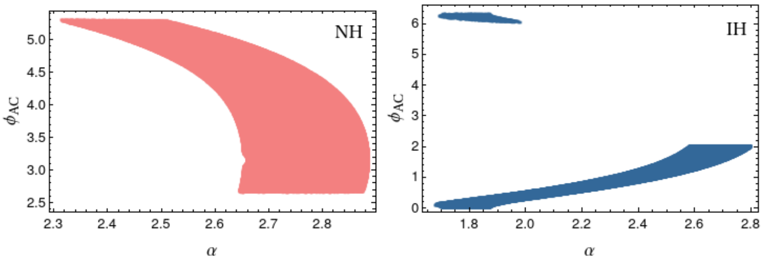

Figure 1: The allowed ranges for α and ϕ_{AC} for both normal (left panel) and inverted (right panel) hierarchy of neutrino masses.

Similar to the mixing angles, following the analysis given in [1], we find that the light neutrino masses also depend on the parameters $\alpha, \beta, \phi_{AC}, \phi_{BC}$. Therefore using the 3σ range neutrino oscillation data [19] on $\theta_{12,13,23}$, $\Delta m^2_{21,31}$ we can constrain the above parameters. In Fig. 1 we have plotted the allowed region in the $\alpha - \phi_{AC}$ plane for NH (left panel) and IH (right panel), respectively. Using these constraints on the model parameters, we can further predict $\delta_{\rm CP}$, $\sum m_i$ and $m_{\beta\beta}$ as given in Fig. 2. For discussion of various other phenomenological aspects of the flavor

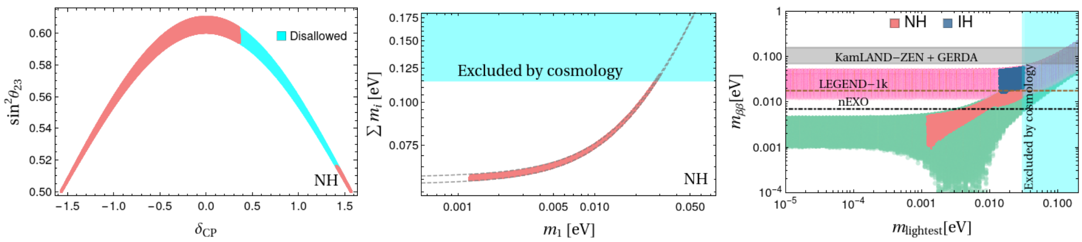

Figure 2: Predictive correlations for $\sin^2\theta_{23} - \delta_{CP}$, $\sum m_i - m_1$ and $m_{\beta\beta} - m_1$ for NH.

symmetric scoto-seesaw model, including LFV decays, see [1].

3. Conclusion

In this work, we have formulated an A_4 flavor symmetric hybrid scoto-seesaw framework to explain neutrino mixing, where both type-I seesaw and scotogenic mechanisms contribute to the effective light neutrino mass. The scotogenic contribution is a common origin of θ_{13} and dark matter. The model is very predictive in nature and exhibits a wide range of predictions. We obtain a lower limit on the lightest neutrino mass as $m_{\rm lightest} \geq 0.0012$ eV for normal hierarchy and $m_{\rm lightest} \geq 0.014$ eV for inverted hierarchy. We have also estimated the prediction for $m_{\beta\beta}$ and found it to be in the range $1 - 30$ meV for normal hierarchy and $16 - 60$ meV for inverted hierarchy, respectively. These values are within reach of future neutrinoless double beta decay experiments.

Acknowledgments

This work has been supported in part by the Polish National Science Center (NCN) under grant 2020/37/B/ST2/02371 and the Freedom of Research (Swoboda Badań) initiative of the University of Silesia in Katowice.

References

[1] J. Ganguly, J. Gluza, and B. Karmakar, JHEP **11**, 074 (2022), arXiv:2209.08610 [hep-ph] .

[2] N. Rojas, R. Srivastava, and J. W. F. Valle, Phys. Lett. B **789**, 132 (2019).

[3] H. Ishimori, T. Kobayashi, H. Ohki, Y. Shimizu, H. Okada, and M. Tanimoto, Prog. Theor. Phys. Suppl. **183**, 1 (2010), arXiv:1003.3552 [hep-th] .

[4] G. Altarelli and F. Feruglio, Rev. Mod. Phys. **82**, 2701 (2010), arXiv:1002.0211 [hep-ph] .

[5] S. F. King and C. Luhn, Rept. Prog. Phys. **76**, 056201 (2013), arXiv:1301.1340 [hep-ph] .

[6] G. Chauhan, P. S. B. Dev, B. Dziewit, W. Flieger, J. Gluza, K. Grzanka, B. Karmakar, J. Vergeest, and S. Zieba, in *2022 Snowmass Summer Study* (2022) arXiv:2203.08105 [hep-ph] .

[7] D. Borah and B. Karmakar, Phys. Lett. **B780**, 461 (2018), arXiv:1712.06407 [hep-ph] .

[8] D. Borah and B. Karmakar, Phys. Lett. B **789**, 59 (2019), arXiv:1806.10685 [hep-ph] .

[9] D. Borah, B. Karmakar, and D. Nanda, JCAP **07**, 039 (2018), arXiv:1805.11115 [hep-ph] .

[10] S. F. King, JHEP **08**, 105 (2005), arXiv:hep-ph/0506297 .

[11] P. F. Harrison and W. G. Scott, Phys. Lett. **B535**, 163 (2002).

[12] B. Karmakar and A. Sil, Phys. Rev. **D91**, 013004 (2015), arXiv:1407.5826 [hep-ph] .

[13] B. Karmakar and A. Sil, Phys. Rev. D **93**, 013006 (2016), arXiv:1509.07090 [hep-ph] .

[14] B. Karmakar and A. Sil, Phys. Rev. D **96**, 015007 (2017), arXiv:1610.01909 [hep-ph] .

[15] S. Bhattacharya, B. Karmakar, N. Sahu, and A. Sil, Phys. Rev. D **93**, 115041 (2016), arXiv:1603.04776 [hep-ph] .

[16] S. Bhattacharya, B. Karmakar, N. Sahu, and A. Sil, JHEP **05**, 068 (2017), arXiv:1611.07419 [hep-ph] .

[17] E. Ma, Phys. Rev. D **73**, 077301 (2006), arXiv:hep-ph/0601225 .

[18] D. M. Barreiros, F. R. Joaquim, R. Srivastava, and J. W. F. Valle, JHEP **04**, 249 (2021), arXiv:2012.05189 [hep-ph] .

[19] P. F. de Salas, D. V. Forero, S. Gariazzo, P. Martínez-Miravé, O. Mena, C. A. Ternes, M. Tórtola, and J. W. F. Valle, JHEP **02**, 071 (2021), arXiv:2006.11237 [hep-ph] .